Original Article

Evaluating the advantages of Image based Shoreline Change Detection Analysis over Traditional GIS based Shoreline Change Detection Method (DSAS)

Perumala Susmitha[1], Dr. S. Narayana Reddy[2]

[1]*Research Scholar, Sri Venkateswara University College of Engineering, Department of ECE, Tirupati, Andhra Pradesh, India*

[2]*Professor, Sri Venkateswara University College of Engineering, Department of ECE, Tirupati, Andhra Pradesh, India*

Abstract: *The current study is an evaluation and comparison of the conventional GIS based shoreline change analysis and using the change detection techniques using image-processing method. The study area chosen is 253 km long coast along the districts of Kakinada, and Visakhapatnam, Andhra Pradesh, India. The coast is very dynamic environment, with the Godavari River in the southern-most part delivering many sediments, and many tropical cyclones affecting the area almost every year. The shoreline change performed through Digital Shoreline Change Analysis (DSAS) in the more common and conventional way and serves as the baseline for comparing the image-based shoreline change, from the change detection method. The study shows that the Image based method is reliable for a region where the coast does not have much of wave action to measure the change detection precisely and faster. However, for a more accurate measurement, and for regions where manual intervention and interpretation were required, the conventional GIS based analysis is more suitable.*

I.INTRODUCTION

The coast is a dynamic morphological entity, which is continuously influenced by external forces, such as waves, tides and currents near the coast (Fig 1). This results in the transport of sediments and if the resulting sediment transport to a given area is greater than the sediment transport away from that area, results in accretion or beach development (Baily and Nowell, 1996). Conversely, when there is a deficit of incoming sediment supply compared to outgoing sediment supply, erosion occurs (Mani Murali et al., 2009). It takes several months or years to observe the impact of this erosion and deposition, hence it is called "long-term coastal hazard" (Prasad and Kumar, 2014). Consequently, it causes a serious threat to coastal environment, human life,and property.
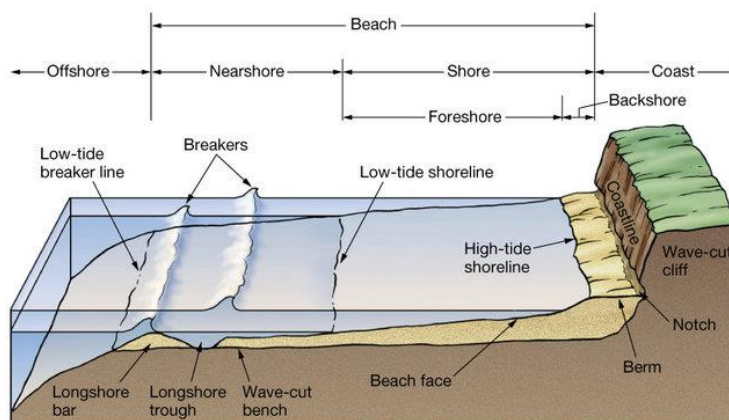

Figure 1:Physiography in the coastal environment (Hamson, 1988)

Shoreline change is one of the most frequently affected parameters owing to natural hazards and it is widely researched coastal issues in the world as it changes shape and position over multiple spatial and temporal scales

(Burningham et al., 2020). Therefore, shoreline changes are therefore required to identify the processes that caused these changes in any specific area, to assess human impact and to plan management strategies (Adarsa et al., 2016). Remote sensing data is very useful to observe the coastal zones changes including the shoreline with good accuracy (Kannan et al., 2016). Since remote sensing data has high resolution, multispectral capabilities, providing a much-needed temporal coverage of any given region, it renders very useful to observe the coastal zones changes including the shoreline with good accuracy (Lillesand et al., 2015; Cendrero, 1989).

Many articles deal with coastal behaviour and applied coastal research. (Shalowitz, 1964) examined the determination of marine boundaries in the United States and expanded on the key principles of coastal studies. (Andrews et al., 2002) described basic ideas for applying GIS tools to predict coastal sediment behaviour and emphasized the need to understand sand flows in a coastal environment Morton and White (1995) discussed erosion processes based on geological differences in shoreline components and stressed the critical need to establish a link between shoreline types and erosion rates. Seasonal variations and the consequences of episodic and extreme events such as storms, floods and hurricanes have been the subject of short-term research. Because of the greater amount of energy that can be released by factors such as high-speed winds, flood discharges, large waves and storm surges, violent events can cause more significant changes to the coast than the cumulative effect of long-term fluctuations. Douglas and Crowell (2000) also discussed the importance of forecasting coastal positions for more effective coastal management.

Changes in shoreline position can have a significant impact on human activities Frihy and Lotfy (1994). The installation of heavy equipment and permanent infrastructure (such as roads and ports) along unstable coastlines, the mining of underground resources in areas prone to subsidence, and the development of industries and housing in environmentally sensitive areas are examples of human societies having negative impacts. Coastal processes cannot be tamed and need to be better understood, as evidenced by the recurring damage or destruction of infrastructure and the continued depletion of resources to consolidate vulnerable defences. Researchers were able to use these digital datasets to develop coastal behaviour models to identify erosion-prone regions along the coast, identified by average annual erosion rate (AAER)-based thresholds. Using rates of change as an indicator of shoreline dynamics, historical shoreline data can be used to determine the primary shoreline processes at work in particular shoreline regions. Coastal behaviour needs to be studied to avoid previous mistakes and to ensure that the optimal applications are selected for each site. This study is an attempt to compare the use of traditional GIS-based shoreline survey versus image-based shoreline detection (Parthasarathy et al., 2018). The purpose of this study is to evaluate the advantages and disadvantages of both methods to extract the coast change analysis.

II.STUDY AREA

The study area taken for evaluation is the coastal region in the north of Godavari River. The coast in the study area passes through the districts of Kakinada and Visakhapatnam and the total coast length is ~253 km, excluding the ports, and the sand bars duly developed (Fig 2). The nearby places are marshy wetland, also home to India's second largest mangrove forest and the Coringa Wildlife Sanctuary. A branch of the Godavari River, the Gouthami, flows into the Bay of Bengal in the study area.
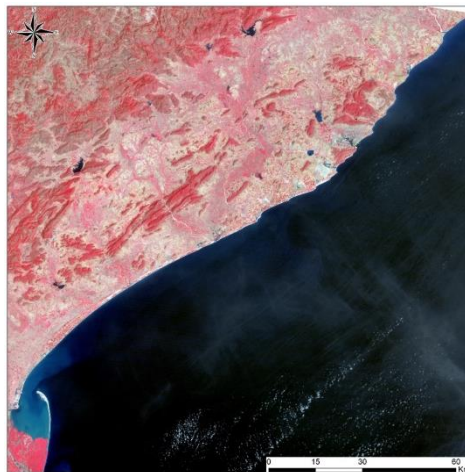

Figure 2:standard fcc of oli data, showing the full length of the coast taken for the Current Study.

III. DATA AND METHODOLOGY

This study has used the Multi-Resolution and Multi-Temporal satellite data of Landsat TM and OLI/TIRS. These datasets were obtained on free from clouds or with minimum cloud days of different dates over the taken period (1988 to 2021). Methodology for this study has divided into several parts about the technique and methods for each data. Data collected are from both LANDSAT 5 and LANDSAT 8, depending on the data availability. Landsat 5 TM satellite datais having seven spectral bands with the resolution of 30 meters for band 1 to 7 (Band 6 was collected at 120m (Thermal

infrared band), it is resampled to 30meters) (Phiri and Morgenroth, 2017) Whereas Landsat 8 OLI/TIRS image data files consist of eleven spectral bands. The resolution 30 meters for band 1 to 7, 15 meters for band 8 (panchromatic band), 100 meters for band 10 and band 11 (Thermal infrared band). For the period of 1988 to 2011 LANDSAT 4-5 TM Level-1 imageries are collected, and from 2014 till 2021, LANDSAT 8 OLI/TIRS C1 Level-1 imageries are collected from the USGS website. The dates of the data collected are given in Table 1.

Table 1: Table depicting the year, month and sensor of the datasets used for the study.

Sensor	Spatial Resolution	Year	Month
Landsat 5 TM	30	1988	March
Landsat 5 TM	30	1992	March
Landsat 5 TM	30	1996	March
Landsat 5 TM	30	2001	February
Landsat 5 TM	30	2005	April
Landsat 5 TM	30	2008	April
Landsat 5 TM	30	2011	March
Landsat 8 OLI/TIRS	30	2014	March
Landsat 8 OLI/TIRS	30	2018	March
Landsat 8 OLI/TIRS	30	2021	March

A. Data Acquisition

Data acquisition is a critical step in change detection research, particularly coastal change. The acquisition period (i.e., season, month) of multi-date images can affect the coast due to the swelling and sinking of the sea, thus changing the coast seasonally. The moon phase also influences the coastline at high and low tide. "However, data selection is often limited by data availability, and the choice is usually a trade-off between target period, collection interval, and data availability." So, while there is a wealth of data available for each season, the same cannot be said for the effects of lunar tides. Careful selection of images from multiple dates is necessary to minimize the impact of seasonal effects of climatic conditions. The acquisition interval between the multi-data imagery is also important to be considered, since the earth's surface causes radiative changes to be observable. In this study, the datasets range from 1988 to 2021, most of which were acquired in March, to avoid seasonality, using the same month or season. Moreover, the monitoring interval was chosen to be 3-4 years, so the trend of changes is easy to understand.

B. Image Processing

To successfully demarcate the shoreline through image processing, the image needs to be subjected for a set of manipulations, which are executed in the ERDAS 2014 image processing software.

a. DN To TOA Conversion

Before the data can be used for data classification or ratioing, the raw DN values need to be converted to TOA reflectance, which is a two-step process, involving DN to at-sensor Radiance conversion, followed by at-sensor radiance to top-of-the-atmosphere conversion. "The need of at-sensor spectral radiance conversion from DN is to convert the multiple sensors image data into common radiometric scale, and after this conversion the image data has to be converted TOA reflectance, as there are few advantages to using TOA reflectance instead of at-sensor spectral radiance, it includes removing cosine effect, correcting the Earth-Sun distance between different data acquisition dates."

b. Classification

The next step is to classify the image into two classes, one is water, and other is everything else. This is achieved by using both parametric and non-parametric classifiers. The parallelepiped classifier is also called as box classifier, which is a supervised classification algorithm. It uses simple logic rule-based algorithm. The signature file of the classes is given by the analyst, which decides the given pixels are within class or not by comparing with the threshold value. As the analyst is deciding the training selection. So, this parallelepiped classifier is in supervised classification. "For all the bands in the multispectral images, a valid range intensity values are specified by a minimum member of a class if and only if all its band information or signature falls within corresponding ranges of the bands defined by that class. A pixel can be classified to class 1, that its signature falls within that range. Unclassified pixels are assigned to a designated class (e.g., class 0)." The Spectral Angle Mapper (SAM) algorithm Xiaofang Liu and Chun Yang (2013) widely used for remote sensing images, which is a supervised classification algorithm. "SAM algorithm assigned various classes based on the spectral angle. The spectral angle is calculated between the test vector built for each pixel and the reference vector built for each reference classes selected by the user. However, when threshold for classification based on spectral angle is modified, the

probability of incorrect objection detection may increase. The SAM algorithm is a linear model which does not work when the classes are overlapped with each other (Rashmi et al., 2014).

c.Change Detection

The process of recognising differences in the condition of an object or phenomenon by watching it at different times is known as change detection (Ashbindu, 1989). The timing and accuracy of detecting changes on the Earth's surface can provide insight into the relationship and interaction between human and natural phenomena. The different applications are involved in change detection techniques such as coastal monitoring, deforestation, urban development, damage assessment and planning and land layout.

IV.DIGITAL SHORELINE ANALYSIS SYSTEM (DSAS)

Digital Shoreline Analysis System (DSAS) was used for measuring the conventional change detection using GIS methods. DSAS is an add-on for ESRI ArcGIS package that calculates the rate-of-change data from shorelines. DSAS computes change rates of end point rate, simple linear regression, weighted linear regression, and least median of squares. All these calculations have their own advantages and needs to be implemented appropriately. The results of all rate calculations are output to a table that can be linked to the transect file by a common attribute field. The software can also be used to find changes of glacier, river edge boundaries, land use land cover changes etc. (Thieler et al., 2009). This tool, developed by the United States Geological Society, has aided in the analysis of coastline change in all coastal locations throughout the world. This module allows you to generate perpendicular baseline transects along the shore at the user-specified spacing (Fountoulis et al., 2015).

While manually digitizing, three ports along the coast viz. Visakhapatnam, Gangavaram and Kakinada ports were ignored as they were developed along this period (1988-2021) and any result that is obtained will be "false value", due to the high anthropogenic intervention. The river mouth of Godavari was also excluded from this study as it is very dynamic and does not contribute to the coastline changes in a sense of consistency. "A theoretical baseline at 200 m distance was created using ArcGIS behind the shorelines using copy parallel tool. The tool records shoreline changes by measuring the distance between the baseline and the shoreline locations. Then, along the coastline, DSAS constructs transects that are set perpendicular to the baseline at the user-specified user specified spacing (Fig 3)." "The DSAS tool is used to produce a total of 9914 transects down the shore that are perpendicular to the baseline and spaced at 25 m intervals." The spacing of 25 m was chosen in consideration to the spatial resolution of Landsat MSS, TM and OLI sensors (30 m) and pansharpened OLI image (15m). This utility generates a statistics table that includes all measured distances. This study used an End Point Rate (EPR) statistical technique to track shoreline changes during the chosen 33-year period.

Figure 3: Shorelines Digitized From Multi-Temporal Datasets, With Transects Intersecting Them Perpendicularly

While digitizing the shoreline, the wave effect along the coast (swash and backwash) were carefully avoided. To digitize the shorelines, the aid of band ratio was taken in addition to the classic visual interpretation method, as a double check. PAN-Sharpened data was also used from the OLI sensor data, for mapping at a higher accuracy. The digitization was done based on visual interpretation of the satellite imageries. Various band combinations were used, viz True colour composite (Landsat 8- RGB: 4-3-2; Landsat 5- RGB: 3-2-1) and False colour composite (Landsat 8- RGB: 5-4-3; Landsat 5- RGB: 4-3-2). There were certain challenges faced while digitizing, for example, the colour tones of land and wave

action would be similar, in this case band ratio technique is used to differentiate water and land, the band ratio NIR/Red (Landsat 8 - Band5/Band4; Landsat 5 - Band4/Band3) was used.

The vectorized shoreline in the 1988 imagery (actual baseline) was utilised to build and calculate the polygons in the Change Polygon Method. The baseline, the shoreline of the year of interest, and two orthogonal to the baseline lines that limited the area under research (closure lines) were all included in each step. The northern, central and southern boundaries of the study area were marked with these closure lines. Perpendicular lines that limit the region (closure lines) must intersect both the baseline and the line of the year of interest in order to form a polygon between the date under investigation and the base line, which is required for the method's application. The change polygon method was used to calculate changes for the period of 1988-2011 (Landsat 5 series), 2014-2021 (Landsat 8 series) and 1988-2021 (entire timescale). To compute the eroded area, the polygon resulting from the oldest date was subtracted from the one resulting from the most recent date in each interval under consideration. The final area value in square metres indicated the eroded area during that time period (Albuquerque et al., 2013). To compute the accretion area, the polygon resulting from the oldest date was added from the one resulting from the most recent date in each interval under consideration.

V. RESULTS AND DISCUSSION

The coast can be split into three zones depending upon the changes observed. The north zone (68.195 km long) (Fig 4 a, b), where there is a head-bay formation, the middle region (90.174 km) (Fig 4 c, d), where there is not much of a drastic change and only some minor accretion, and erosion throughout the stretch and, south zone (94.164 km) (Fig 4 e, f), where there is high erosion and accretion. This split is based on the results of DSAS analysis, as it is the conventional system taken as reference to compare the image difference-based results. A total of 7.26 sq.km. area is eroded in the study area. Of this area eroded, about 50% of the erosion in area, in observed in the south zone, adding up to 3.67 sq. km. The same region also accounts for 8.46 sq. km. of accretion of the 8.81 sq. km of accretion in the whole coast. This is about 96% of the total accretion happened in the complete stretch of the coast. This is a very dynamic change, considering this all has occurred within the same region. This change can be attributed to one major morphological feature in the offshore, which is the spit bar. The spit bar seen in the region is about 16 km in length and is at 12 km off the coast. This spit bar, acts as a barrier from the littoral currents which is flowing towards north from January to October, distributing the sediments while doing so. The littoral current, in combination with the sediment supply of the Godavari River has led to the growth of the spit bar. The spit bar growth is explained in further sections. The barrier has caused the region to be quiet in comparison to the remainder of the coast, causing the mangroves to grow extensively offshore than the other regions. Once protection from the spit bar ends, the littoral currents move aggressively towards the on-shore region, causing severe erosion, which is only natural, and expected. There is however a minor erosion within the spit bar bounded region, which could be a temporary change.

The middle zone, is not having much changes, and only eroded 1.23 sq. km. for a very long stretch of 90.174 km. the total accretion measured in the middle zone is 2.64 sq. km. The values of erosion and accretion for the zones are given in Table 2. The northern zone has developed some interesting features of headland and bay forming alternate regions of high erosion and accretion or equilibrium zone. This alternating erosion and accretion can be attributed to the surface and subsurface hard rock formations, protruding into the shore. These hard rock formations are resistant to erosion, and sometimes act as barrier to the littoral current sediment distribution. Once the barrier of the hard rock ends, the littoral currents head to the northern region aggressively, like the spit bar scenario, and thus eroding and creating small bays. This indicates that there is a dynamic zone in the north and south that needs continuous monitoring, for any future prediction, or mitigation purposes. The middle zone however needs only minor monitoring, since it is not highly active in changing the coastal dynamics.
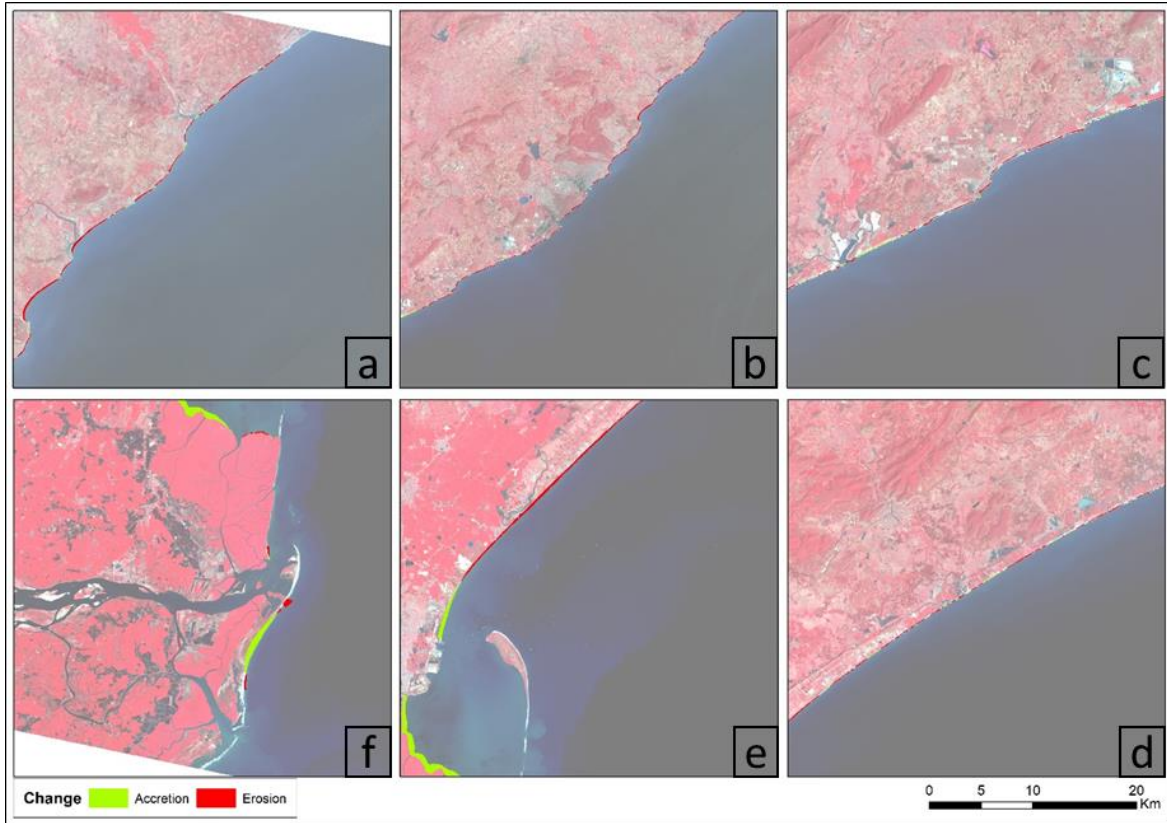
***Figure 4**: Changes in the shore as measured by DSAS, depicted for the net change in the shore. Images placed in clockwise starting at a through f, where a is the northern most extent of coast, and f is the southern-most extent of the coast. Note that the FCC image brightness is reduced to enhance the displayed change analysis results which is otherwise indistinguishable.*

Table 2: Area of accretion and Erosion as per the zones derived from the DSAS results.

Zone	Total Length (Km)	Accretion Area (sq. Km)	Erosion (sq. Km)
Northern Zone	68.195	0.102	2.35
Middle Zone	90.174	0.253	1.26
South Zone	94.164	8.46	3.65
Total Length	252.533	8.815	7.26

The change detection analysis in the image processing method is a straight forward raster subtraction of the classification results of the recent (after) and the older (before) images (Fig 5). Classification of the LANDSAT datasets for the years 1988, 2011, 2014, and 2021 (Fig 5 a, d, g, j) were done by using both non-parametric classifier (parallelepiped) and parametric classifier (SAM). The results were re-coded in the ERDAS Imagine software (Fig 5 b, e, h, k). The images were recoded later as water body, and all the other features as another class (Fig 5 c, f, i and l), since the change of any feature to water body will be erosion, and waterbody changing to any other feature indicates accretion. Differences were done for 1988-2021 (Fig 6), 1988-2011 (between TM datasets) and 2014-2021 (between OLI datasets). The latter two change detections serve as internal checkpoints to make sure that the difference observed is not affected by difference in sensors (TM and OLI). To avoid conflict in the area of change detected by methods, a buffer zone of 200 meters was created from the 1988 shoreline, which is taken as the baseline, from which any and all changes are to be measured. This limit of 200 m was taken so that, there is no drastic difference in the area identified in both methods. Secondly, this buffering distance also makes sure that the inland water bodies close to the coast does not get included in the area calculation. Both the raster-based changes and the vector-based changes were clipped, and area of change is measured. Of the available pixels after clipping, the pixels that has been converted to or from the water bodies multiplied by per pixel area gives the total area that has changed (Table 3).
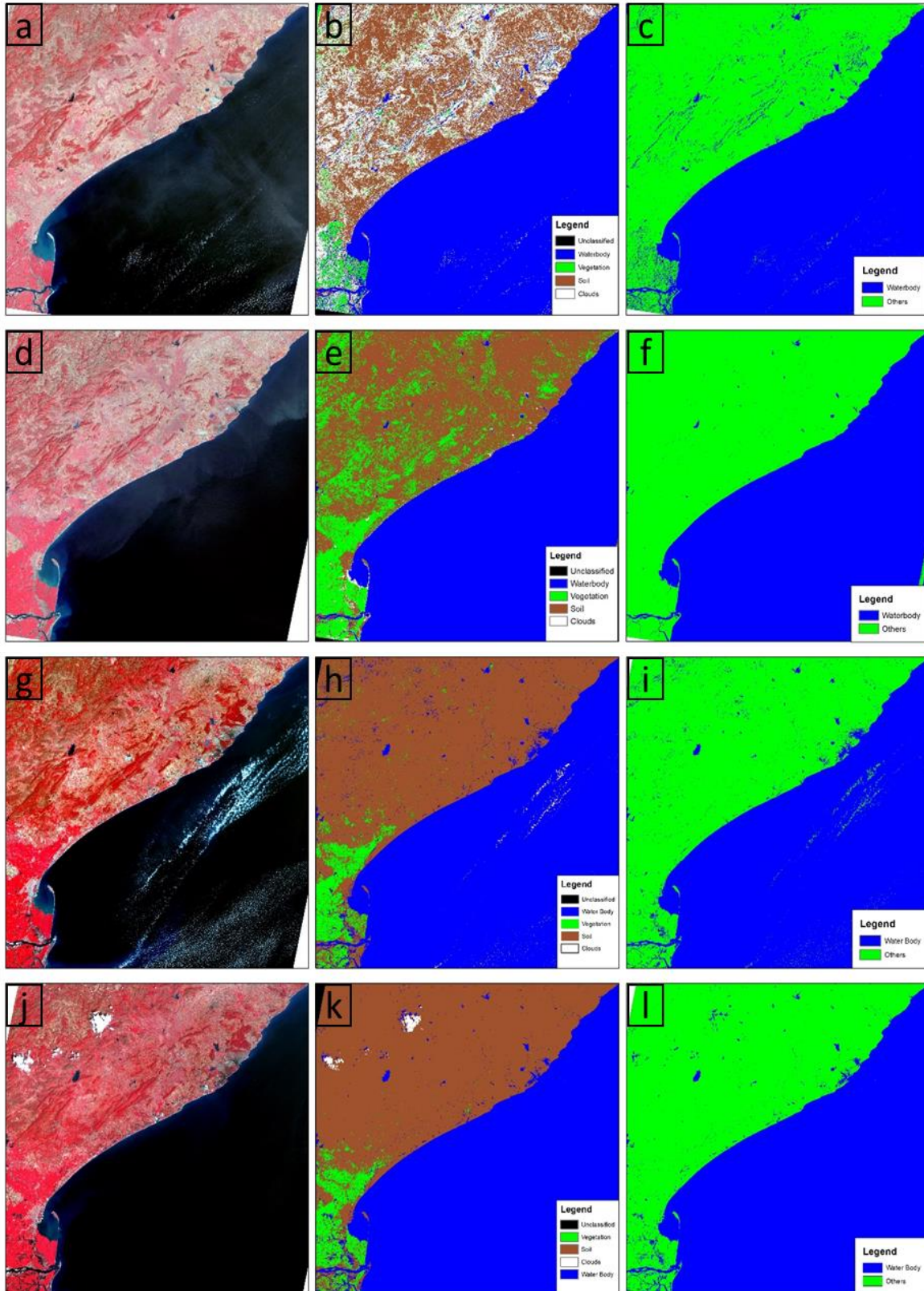
Figure 5: The images used in the classification and image difference, classification results, and the recoded results for the years 1988 (a, b, c), 2011 (d, e, f), 2014 (g, h, i), and 2021 (j, k, l). It is to be noted that the 1988 TM data has a different coverage extent than its 2011 counterpart, as well as the 2014 and 2021 OLI datasets. Also, the classification result of 1988 (4.b) has a lot of mixture within features. But since the objective of differentiating water body from other features was not hindered, the results were taken without much refinement. Same is the case for all the classification results (e, h, k).
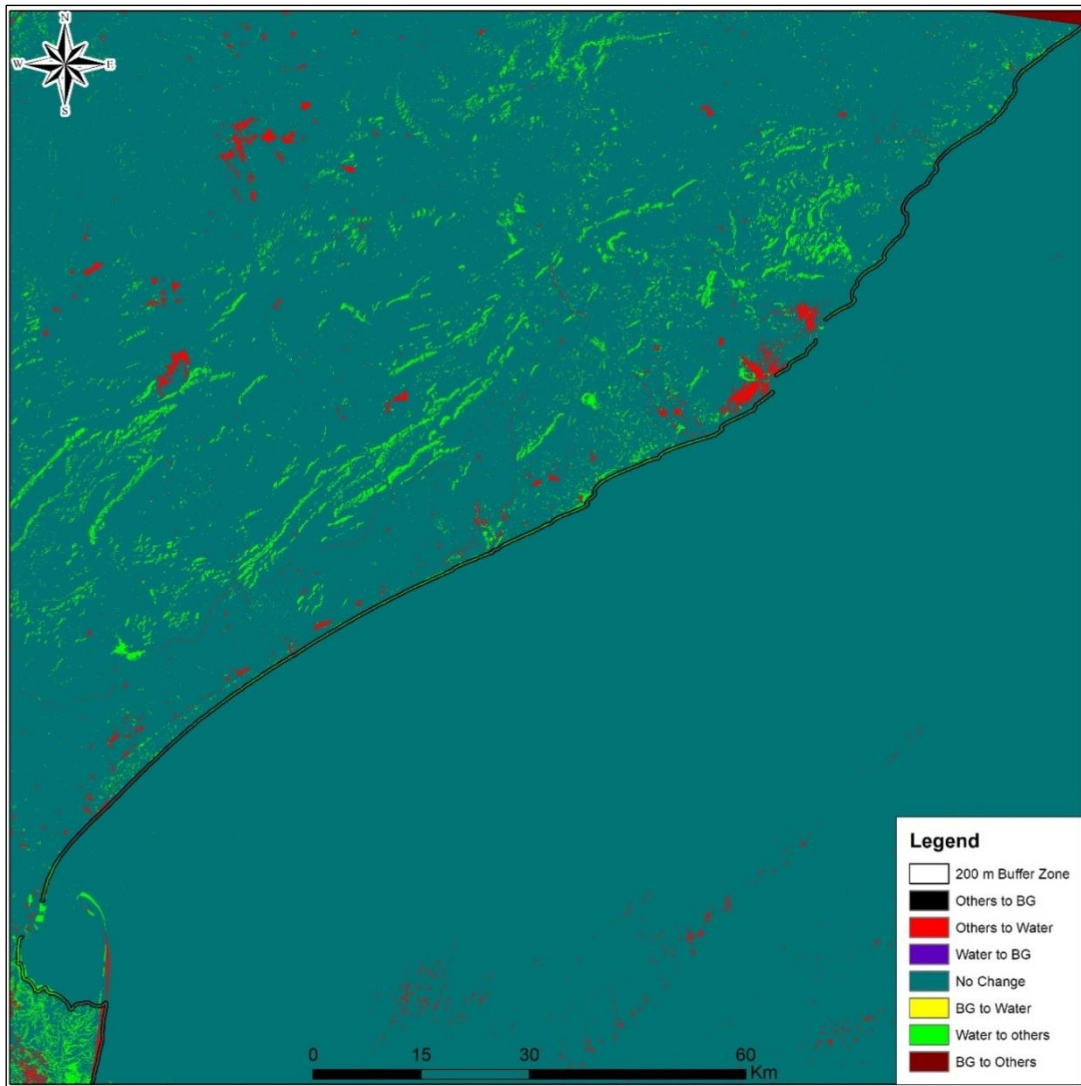
Figure 6: Change Detection output for the net change in the study area (1988-2021). The 200 m buffer of the 1988 shoreline is overlaid on the difference image, the extent of which is only taken for further interpretation.

Table 3: Comparison of results of the Area of Accretion and Erosion from the DSAS and the Change Detection Method

S.no	Change	Area (sq. Km.) (Change Detection)	Area (sq. Km.) (DSAS)	Total Length (km)
1	Accretion	18.9099	8.814803	48.602
2	Erosion	6.8382	7.260129	143.364
3	No change (length only)	N/A	N/A	63.704

The total area taken into consideration after the clipping is 103.06 sq. km. The image difference method shows huge area of accretion (18.91 sq. km.) than erosion. The major portion of erosion is observed in the immediate north of the Kakinada port, where there is a significant spit bar in the offshore region. Otherwise, the results show accretion in general. The accretion also is shown in two stepwise alternating patterns (Fig 7). There is an accretion zone, followed by no change or equilibrium zone, and then again, an accretion zone as one moves from the offshore region to onshore region, perpendicularly. This is quite anomalous from what is expected in shoreline changes. When looked closely what is noted as accretion in the offshore region is not necessarily an accretion, but it is the wave swash and backwash, that is taken by the classification as other features instead of classifying it as waterbody. This means that the waves dimensions vary along the shore as well as away from the shore, at any time, and thus gets recorded where they are present when the data is acquired. Thus, naturally a coast with dynamic wave action should be expected to produce such anomalous result in case of an image-based change analysis. This is also the main reason that though many datasets were downloaded and processed for the analysis, in both DSAS, and image processing methods, that those results are not shown in here. The region where the

Kakinada port is located is comparatively of less waves, which is to be attributed to the 15 km long spit bar formed from the high sediment supply of the Godavari River. The spit bar forms a natural barrier for the littoral currents thereby causing very low disturbance or wave action. Hence in this region, the results are proper, and does not cause any anomalous changes as seen in the northern parts. The growth of mangroves in the south of the Kakinada port is recorded in the image-based change detection. Also, in many places, where the wave activity is very minor, the erosion and accretion processes results from both DSAS, and the image-based change detection matches well, but in a very localized pockets, as given in Fig 8.
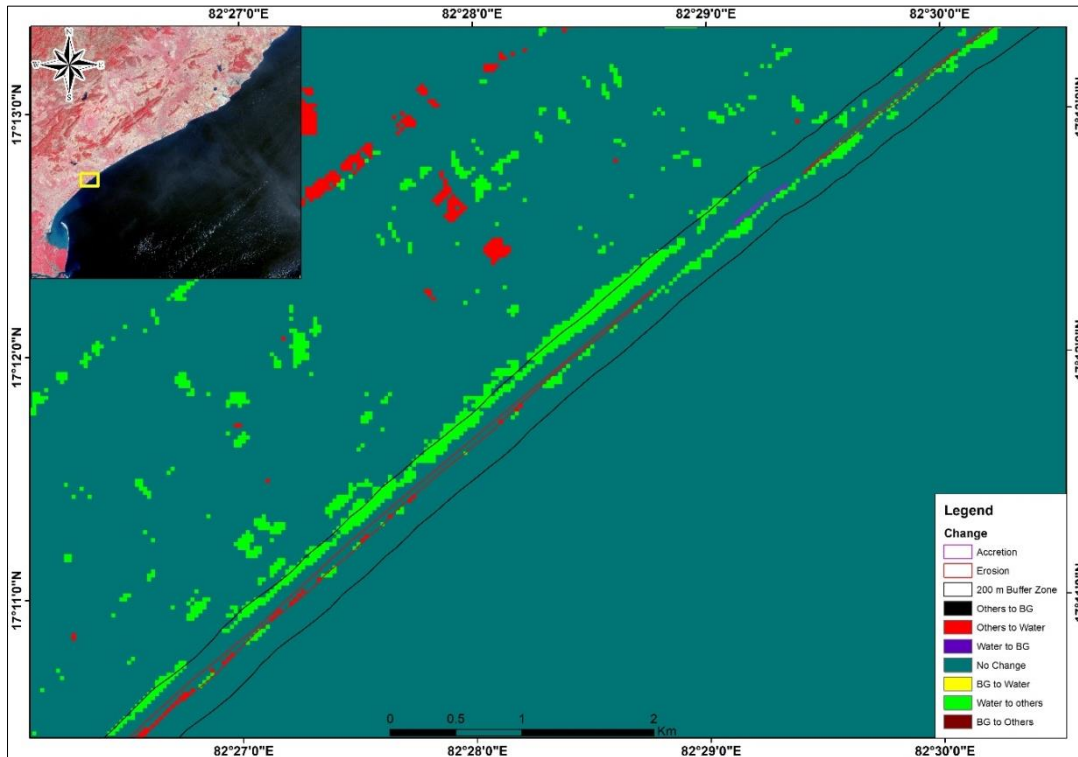

Figure 7: Image showing the accretion in change detection as a stepped result. One in the offshore, and another in the on shore, before and beyond the actual changes marked by hollow polygons, derived from DSAS results.
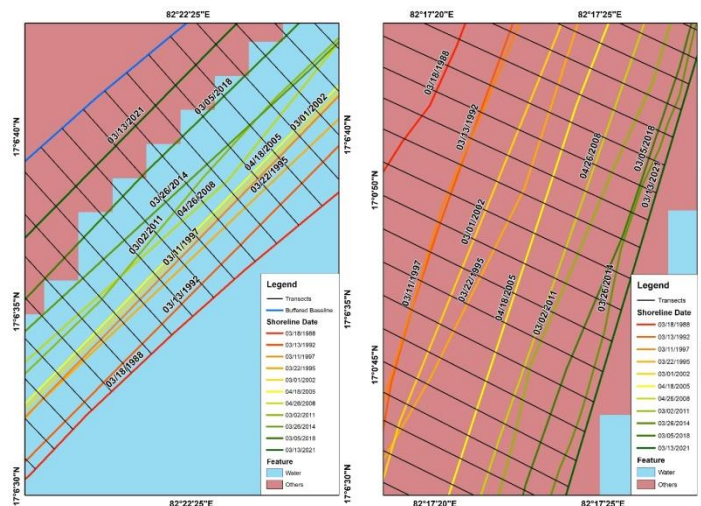

Figure 8: a) Image depicting the erosional environment clearly captured in the image difference process, as well as the GIS based Shorelines mapped. b) Image depicting the accretion being captured clearly by both image difference as well as the GIS based mapping. The shoreline dates are given from 1988 till 2021for reference.

VI. CONCLUSION

Comparing the results of the shoreline change from the image difference and DSAS, it can be observed that there is a lot of contradiction on the surface. But looking in close inspection, the cause could be understood why there is a difference in the change observed with both the methods. The GIS based shoreline has a complete control of the user intervention. It is

highly time consuming, but gives a far better result, whereas the image-based change detection gives a quick result but the result needs proper interpretation, before being taken into consideration or finalizing. The image-based change detection however can be used for inland water bodies, or sea surfaces where the effect of wave is less dynamic.

Interest Conflicts:
The authors declare that they have no known competing financial interests or personal relationships that could have appeared to influence the work reported in this paper.

VII. REFERENCES

[1] Adarsa Jana, SabyasachiMaiti&Arkoprovo Biswas. Analysis of short-term shoreline oscillations along Midnapur-Balasore Coast, Bay of Bengal, India: a study based on geospatial technology. Modeling Earth Systems and Environment, 2016,

[2] Albuquerque, Miguel, et al. "Erosion or coastal variability: An evaluation of the DSAS and the change polygon methods for the determination of erosive processes on sandy beaches." Journal of Coastal Research 65 (10065) (2013): 1710-1714.

[3] Andrews B., P Gares and J. Colby. 2002. Techniques for GIS modeling of coastal dunes. Journal of Geomorphology 48: 289-308.

[4] Ashbindu Singh. Review Article Digital change detection techniques using remotely-sensed data., International Journal of Remote Sensing., 1989, 10, 989-1003.

[5] Baily B, Nowell D., Techniques for monitoring coastal change. Ocean and Coastal Management 2., 1996, 32, 85-95.

[6] Bush, D., R. Webb, L. Hyman, J. Liboy, and J. Neal. 1995. Living with the Puerto Rico Shore, 214 Geomorphology of Puerto Rico, Duke University Press, Durham, NC.

[7] Bush, M. David, O. Pilkey Jr., and W. Neal. 1996. Living by the Rules of the Sea. 179. Living with the Shore, Duke University Press, Durham, NC.

[8] Cendrero A. Mapping and evaluation of coastal areas for planning., Ocean and Shoreline Management, 1989, 12, 427–462.

[9] Darius Phiri and Justin Morgenroth. Developments in Landsat Land Cover Classification Methods: A Review., Remote Sens. 2017, 9, 967.

[10] Dolan R., B. Hayden and J. Heywood. 1978. A new photogrammetric method for determining shoreline erosion. Coastal Engineering, 2: 21-39.

[11] Dolan R., M. Fenster and S. Holme. 1991. Temporal analysis of shoreline recession and accretion. Journal of Coastal research 7(3): 723-744.

[12] Dong P. and H. Chen. 1999. A probability method for predicting time dependent long-term shoreline erosion. Coastal Engineering 36: 243-261.

[13] Douglas B., M. Crowell and S. Leatherman. 1998. Considerations for shoreline position prediction. Journal of Coastal Research 14(3): 1025-1033. Douglas B. and M. Crowell. 2000. Long-term shoreline position prediction and error propagation. Journal of Coastal Research 16(1): 145-152. Duffy W. and S. Dickson 1995. Using grid and graph to quantify and display shoreline change. White paper, Maine Office of Geographic Information Systems, Augusta, Maine.

[14] Fanos A., A. Khafagy, and R. Dean. 1995. Protective works on the Nile delta coast. Journal of Coastal Research 11: 516-528 FEMA. 2000. Evaluation of Erosion Hazards, Summary. Federal Emergency Management Agency. http://www.fema.gov/pdf/hazards/hnz_erosn.pdf accessed July 8, 2003

[15] Fenster M., R. Dolan and J. Elder. 1993. A new method for predicting shoreline positions from historical data. Journal of Coastal Research 9(1): 147-171

[16] Frihy O. and M. Lotfy. 1994. Mineralogy and textures of beach sands in relation to erosion and accretion along the Rosetta promontory of the Nile delta, Egypt. Journal of Coastal Research 10: 588-599.

[17] Fountoulis, Ioannis, et al. "Synergy of tectonic geomorphology, applied geophysics and remote sensing techniques reveals new data for active extensional tectonism in NW Peloponnese (Greece)." Geomorphology 237 (2015): 52-64.

[18] Harman J., 2002. Study suggests many factors affect erosion on beaches with seawalls. Civil Engineering Vol. 72, Issue

[19] Hayes, M. O., 1979. Barrier island morphology as a function of tidal and wave regime. In: S. P. Leatherman (Ed), Barrier Islands from the Gulf of St. Lawrence to the Gulf of Mexico. Academic Press, New York, pp. 1–28.

[20] Helene Burningham, Miriam Fernandez-Nunez. Sandy Beach Morphodynamics., 2020, 439-460.

[21] Kannan R, Ramanamurthy MV and Kanungo A. Shoreline Change Monitoring in Nellore Coast at East Coast Andhra Pradesh District Using Remote Sensing and GIS., J Fisheries Livest Prod 4, 2016, 161.

[22] Mani Murali R, Shrivastava D, Vethamony P., Monitoring shoreline environment of Paradip, east coast of india using remote sensing. Current Science., 2009, 97, 79-84. 23. Mei Xiang, Chih-Cheng Hung ,MinhDinh Pham ,Bor-Chen Kuo and T.Coleman. A parallelepiped multispectral image classifier using genetic algorithms., Geoscience and Remote Sensing Symposium, 2005, 1.

[23] Morelock, J., 1978, Standards for Measuring Shoreline Changes; A Study of the Precision Obtainable, and Needed, in Making Measurements of Changes (erosion and accretion). Coastal Research and the Geology Dept., Florida State University, Tallahassee, Florida, p. 63-64.

[24] Prasad D.H and N.D. Kumar., Coastal erosion studies – a review. International Journal of Geosciences.,2014, 5, 341-345.

[25] Parthasarathy K.S.S., SaravananSubbarayan, Abijith D. Shoreline Change Detection Using Geo-Spatial Techniques- A case Study for Cuddalore Coast., 6th International symposium on Advances in Civil and Environmental Engineering Practices for Sustainable Development, 2018.

[26] Saranya G, Azhagu Kowshik A M, Cibiraj M, Hariharan P, Harish Ramana Kumar G, 2022. "A Deep Learning Model For Brain Tumor Segmentation & Classification Using U-Net & Inception-Net"ESP Journal of Engineering & Technology Advancements 2(4): 20-23.

[27] P Sherman D. and P. Gares. 2000. The geomorphology of coastal environments. Geomorphology 48: 1-6.

[28] Rashmi S, SwapnaAddamani , Venkat and Ravikiran S. Spectral Angle Mapper Algorithm for Remote Sensing Image Classification., International Journal of Innovative Science, Engineering & Technology, 2014.

[29] Shalowitz A. 1964. Shore and Sea Boundaries: U.S. Department of Commerce Publication. Washington DC, 10-1, v.2, 729.

[30] Xiaofang Liu and Chun Yang.a Kernel Spectral Angle Mapper Algorithm for Remote Sensing Image Classification., 6th International Congress on Image and Signal Processing (CISP 2013), 2013, pp. 814-818.